ACS APPLIED MATERIALS & INTERFACES

Letter

www.acsami.org

Preparation and Characterization of Self-Supporting Thermochromic Films Composed of VO_2(M)@SiO_2 Nanofibers

Shaotang Li,[†,‡] Yamei Li,[†,‡] Meng Jiang,[†,‡] Shidong Ji,[†] Hongjie Luo,[†] Yanfeng Gao,[†] and Ping Jin*[,†,§]

[†]State Key Laboratory of High Performance Ceramics and Superfine Microstructure, Shanghai Institute of Ceramics, Chinese Academy of Sciences, Shanghai 200050, China

[‡]Graduate University of Chinese Academy of Sciences, Beijing 100049, China

[§]National Institute of Advanced Industrial Science and Technology (AIST), Moriyama, Nagoya 463-8560, Japan

Supporting Information

ABSTRACT: Nanofibers of VO_2(A) with the diameter and length averagely at 100 nm and 10−20 μm were prepared via a facile one-step hydrothermal method by reducing NH_4VO_3 with 1,3-propylene glycol in an acidic solution. The obtained VO_2(A) was coated by SiO_2 to form VO_2(A)@SiO_2 core−shell nanocomposites, which were then transformed into VO_2(M)@SiO_2 by annealing under nitrogen atmosphere. The resulted composites maintained the original fibrous morphology, particularly with a large amount of pores emerging inside the fiber due to the volume shrinkage during the phase transition, which may improve its thermal insulation ability in real applications. The VO_2(M)@SiO_2 nanofibers were arranged into a self-supporting film by filtration, which shows excellent thermochromic properties.

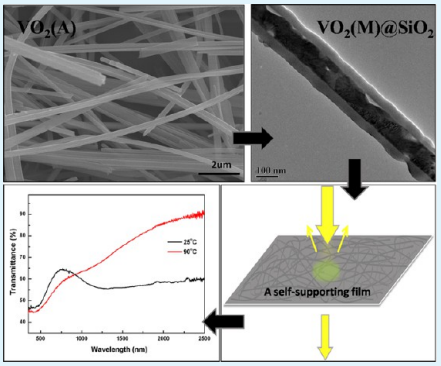

KEYWORDS: *VO_2(M)@SiO_2, nanofibers, thermochromic, self-supporting*

1. INTRODUCTION

Vanadium dioxide (VO_2(M)) has been attracting extensive attentions as a typical thermochromic material. It exhibits thermochromism due to a reversible metal-to-insulator phase transition (MIT) at about 68 °C, accompanied by changes in crystal structure from monoclinic (VO_2(M)) to tetragonal (VO_2(R)).[1,2] The sharp change in optical properties and the fact that the transition temperature can be shifted to room temperature by elemental doping or other multiple ways makes the material one most promising candidate for thermochromic smart window to realize an automatic solar/heat control in response to environmental temperatures.[3] Although thermochromic films have been prepared by a series of methods such as sputtering,[4,5] chemical vapor deposition (CVD),[6] or making flexible foils using VO_2(M) nanoparticles,[7] there have hardly been reports on one-demensional (1D) VO_2(M) nanostructures such as nanofibers or nanowires with large aspect ratio suitable for fabricating self-separating films for special applications.

One-dimensional (1D) nanostructures, such as nanobelts, nanorods, nanofibers, and nanotubes, have raised great attention because of their fundamental research significance and a wide range of potential applications in nanodevices. For the vanadium oxide system, thermochromic VO_2(M) with an elongated 1D morphology should be of the same importance. In fact, it was reported recently that VO_2(M) nanowires could be deposited by chemical vapor transport method (CVT).[8,9] However, such nanowires could only be produced with very small yields just for laboratory research, unsuitable for large scale production for smart window or other real applications.

As the most conventional synthesis method, hydrothermal synthesis method has been applied to obtain nanoscaled vanadium dioxide. However, hydrothermal synthesis resulted in VO_2(M) with morphologies limited to spherical or rodlike ones in most cases because of some crystallographic and thermodynamic causes.[10,11]

However, as a common polymorph of vanadium dioxide, the metastable phase VO_2(B) was often obtained in hydrothermal reaction and revealed nanobelt morphology, which could be precursors to synthesize 1D VO_2(M) by postannealing.[12,13] As another typical VO_2 polymorph, VO_2(A) is more stable and exhibit typically 1D rod/fiberlike morphology, which is very suitable to synthesize 1D VO_2(M) nanofibers by postannealing. The VO_2(A) nanofibers were usually obtained by hydrolysis of tetravalent vanadium compound like vanadyl acetylacetonate,[14,15] or by reduction of V_2O_5,[16] and they were tested as electrode materials for lithium ion batteries recently.[17]

In the present work, VO_2(A) nanofibers were successfully prepared by hydrothermal reduction of NH_4VO_3 in an acidic solution. Preparation conditions such as temperature, reaction time and amount of reducing agent were varied to explore the reaction mechanism and obtain phase pure VO_2(A) nanofibers

Received: May 15, 2013
Accepted: June 22, 2013
Published: June 23, 2013

   dx.doi.org/10.1021/am401839d | ACS Appl. Mater. Interfaces 2013, 5, 6453−6457

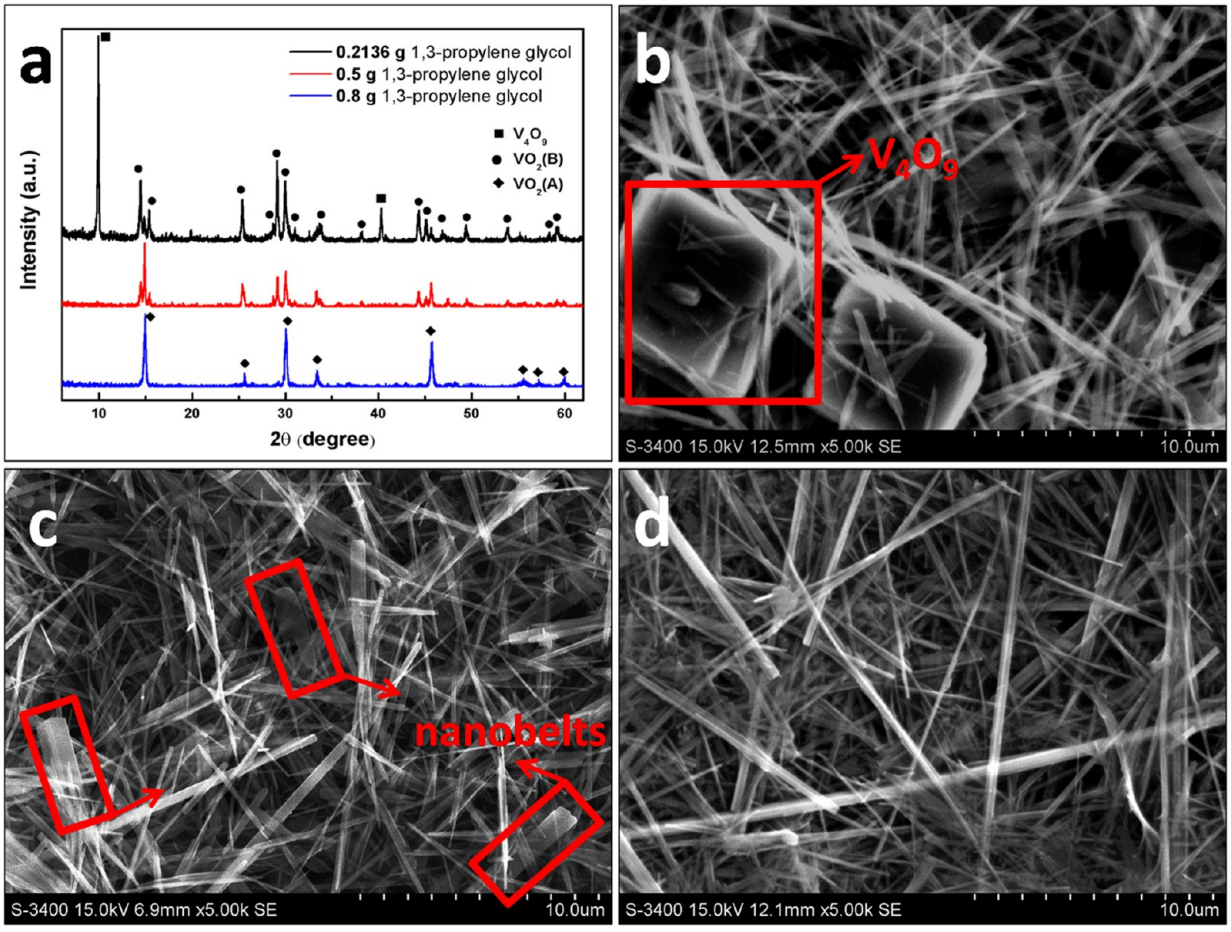

Figure 1. (a) XRD patterns of hydrothermal reaction producst using different amount of 1,3-propylene glycol. (b–d) SEM image of the hydrothermal reaction products using different amount of 1,3-propylene glycol as reductant: (b) 0.2136 g, (c) 0.5 g, (d) 0.8g.

with the largest aspect ratio. A SiO_2 shell was coated on VO_2(A) to get VO_2(A)@SiO_2 nanofibers, and thermal annealing was applied to transform VO_2(A)@SiO_2 into VO_2(M)@SiO_2 without destroying the fibrous feature. Pores was produced inside the fiber because of the volume shrinkage during the phase transition, which may contribute to a better thermal insulation. The VO_2(M)@SiO_2 nanofibers were arranged into a self-supporting film by filtration, which shows excellent thermochromic properties.

2. EXPERIMENTAL SECTION

All reagents were bought from Aladdin Reagent Company (China) and used without further purification. VO_2(A) nanofibers were synthesized by an acid-assisted hydrothermal method. In a typical procedure, NH_4VO_3 (1.8 g), H_2SO_4 (0.8g, 98%), a certain amount of 1,3-propylene glycol, and deionized water (40 mL) were added into a 100 mL Teflon-lined stainless-steel autoclave. The autoclave was sealed and maintained at 240 °C for 24 h. After the hydrothermal treatment, the autoclave was air-cooled to room temperature, and the products were collected by vacuum filtration, washed with distilled water, and dried in vacuum to obtain the VO_2(A) nanofibers.

The SiO_2 coating process was carried out by the modified Stöber method in an ethanol/water solution. In a typical case, 0.2 g of VO_2(A) nanofibers were dispersed in a mixture of alcohol (30 mL), deionized water (10 mL) and ammonia (6 mL), then 300 μL of TEOS was added to the dispersion dropwise under vigorous stirring. The hydrolysis process was kept at 25 °C for 1 h. The products were filtrated, washed with distilled water, and dried in vacuum to obtain the VO_2(A)@SiO_2 nanofibers.

The VO_2(A)@SiO_2 nanofibers were heated in a tube furnace under a flow of nitrogen gas from 500 to 700 °C for 1 h to acquire VO_2(M)@SiO_2 nanofibers. The VO_2(M) nanofibers without SiO_2 coating were also obtained by vacuum annealing the pure VO_2(A) for comparison.

A thermochromic film was prepared by depositing a certain amount of VO_2(M)@SiO_2 nanofibers in water onto a cellulose membrane by vacuum filtration. Heat and pressure were used to make the composite dry and smooth. The composite was put into an atmosphere of acetone vapor until it become transparent, and the remained cellulose was further eliminated by wash with acetone to obtain a self-supporting film composed of VO_2(M)@SiO_2 nanofibers.

The crystal structure of the samples was investigated by X-ray diffraction (XRD; Model D/Max 2550 V, Rigaku). The microstructure was observed with a transmission electron microscope (TEM; JEM-2010F, JEOL) and a scanning electron microscope (SEM; S-4300, Hitachi). The phase transition behavior was studied with differential scanning calorimetry (DSC DSC204F1, Netzsch) performed in nitrogen flow in the range of 0–100 °C with a heating rate of 5 °C min^{-1}. The optical transmittance of the self-supporting film at normal

dx.doi.org/10.1021/am401839d | ACS Appl. Mater. Interfaces 2013, 5, 6453–6457

incidence was measured from 350 to 2500 nm using a Hitachi U-4100 spectrometer.

3. RESULTS AND DISCUSSION

Different amount of 1,3-propylene glycol was tried as the reducing agent to investigate the phase formation and obtain a phase pure VO_2(A) with the expected fibrous structure. The results of the XRD patterns and SEM images were shown in Figure 1. As 0.2136 g of 1,3-propylene glycol was added, the product was a mixture of V_4O_9, VO_2(B), and VO_2(A) (Figure 1a), although the amount is the theoretical one calculated to acquire tetravalent vanadium oxide under a complete reaction. Accordingly, the SEM image in Figure.1b shows two morphologies: a fibrous one and a platelike one, corresponding to the VO_2(B) or VO_2(A) and V_4O_9, respectively. The obvious (200) peak of V_4O_9 correspond to its square and plate morphology.[18] As the 1,3-propylene glycol was increased to 0.5 g, the product becomes tetravalent vanadium oxides composed of VO_2(B) and VO_2(A) with different morphologies (nanobelt and nanofiber, respectibely), as shown in Figure.1c. Further increasing the reducing agent to 0.8 g could obtain a phase-pure VO_2(A) as shown in Figure.1d. The morphology of the phase-pure VO_2(A) is shown in Figure 2 as a enlarged image, which

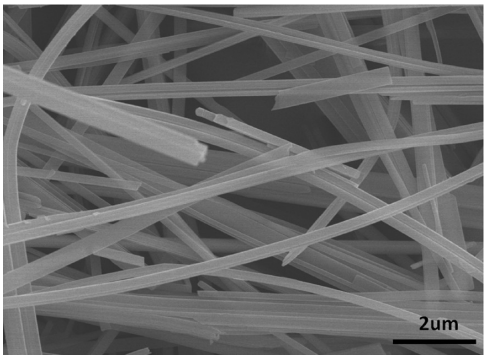

Figure 2. SEM image of VO_2(A) nanofibers by reduction of NH_4VO_3 in acid solution.

clearly proved its fibrous structure with fibers approximately 100 nm in width and up to several tenth of micrometers in length. Further increasing reducing agent did not produce lower valence state vanadium oxide because of the weak reducing ability of 1,3-propylene glycol, showing the advantage for controlling the reaction product. Change 1,3-propylene glycol to other carbon-based organic reducing agents such as formic acid, acetic acid, oxalic acid, ethylene glycol, malonic acid, and polyethylene glycol gave similar results and could obtain a phase-pure and fibrous VO_2(A). It can therefore be concluded that the use of carbon-based organic reducing agents are suitable for producing fibrous VO_2(A) within a wide composition range.

The reaction was also carried out at different temperatures ranging from 180 to 230 °C to study the temperature effect. A mixture of VO_2(B) and VO_2(A) was always formed at the above temperatures when the reaction time was 24 h, indicating 240 °C or higher temperatures were crucial in this reaction to acquire pure VO_2(A). Reaction time was changed to understand the growth mechanism and phase evolution when reaction temperature was 240 °C (see Figure S1 in the Supporting Information). After 8 h, V_4O_9 and VO_2(B) both existed and VO_2(B) nanobelts were as long as 6 μm. While at the 14 h VO_2(B) nanobelts did not grow longer but partly converted to VO_2(A). The agglomerated nanowires should be VO_2(B) or VO_2(A) that had just split from V_4O_9. Some small and thin crystals in Figure S1b in the Supporting Information revealed VO_2(A) nanowires were mainly generated from nucleation and growth rather than assembled from VO_2(B) nanobelts. Small amount of VO_2(B) nanobelts remained while the VO_2(A) nanowires grew to more than 10 μm. Pure VO_2(A) was obtained after 24 h or longer time with the expected fibrous feature; however, the nanofibers appeared not to grow longer but better crystallized at the 40 h. This length seems to be its thermodynamically stable state.

It was reported that VO_2(B) nanobelts could be transformed into VO_2(M) by heat treatment[12,13] (though the original belt-like morphology could not be kept). It was found that our VO_2(A) nanofibers could similarly be completely converted to VO_2(M) by vacuum annealing at 550 °C for 1 h, which was seldom reported (Figure 3). However, annealing of bare VO_2(A) resulted in destruction (broken and agglomeration) of the original fibrous morphology, as shown in Figure 3b. Therefore, SiO_2 coating was used to avoid the destruction of original fibrous form during annealing, as the annealed VO_2(M) @SiO_2 shown in Figure 3c. The SiO_2 coated samples could keep its original fibrous structure even at a high temperature of 700 °C to achieve a complete phase transition. Detailed results of annealing are summarized in Table S1 (see the Supporting Information).

The density values of VO_2(A) and VO_2(M) are 4.035 and 4.67 g/cm^3, respectively. Thus, there should be quite a large

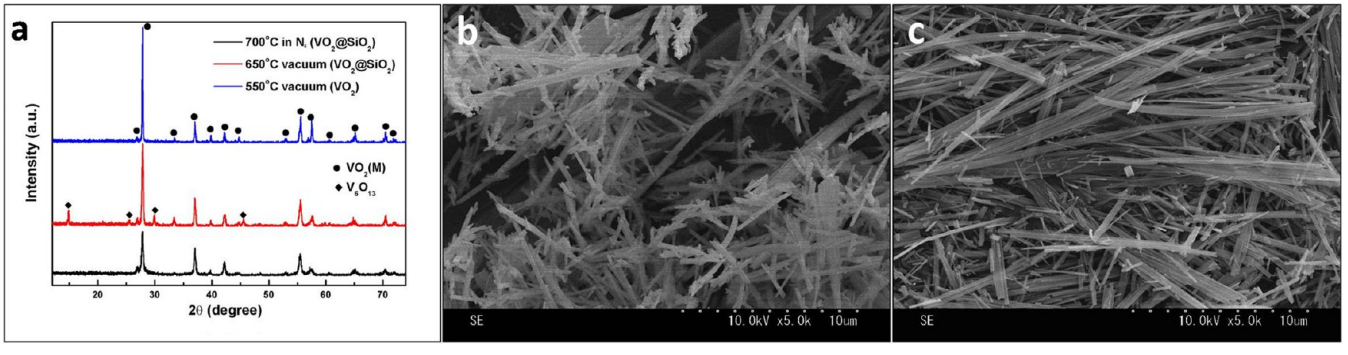

Figure 3. (a) XRD patterns of VO_2 nanofibers and VO_2@SiO_2 nanofibers annealed under different conditions. (b) SEM image of VO_2(M) nanorods obtain by a 550 °C vacuum annealing of VO_2(A) nanofibers. (c) SEM image of VO_2(M)@SiO_2 nanofibers obtain by a 700 °C annealing of VO_2(A) @SiO_2 nanofibers in nitrogen.

dx.doi.org/10.1021/am401839d | ACS Appl. Mater. Interfaces 2013, 5, 6453−6457

volume shrinkage in the transformation of VO_2(A) to VO_2(M) during annealing, which can definitely results in the destruction of the fibrous structure. In fact as shown in Figure 3b, a lot of small grains of VO_2(M) could be seen and the nanofibers became nanorods during annealing of bare VO_2(A) without SiO_2 coating. However, the original fibrous feature was kept by the VO_2(M)@SiO_2 structure as shown in Figure 3c. Meanwhile, other advantages such as antioxidation and antiacid abilities of VO_2(M) can also be expected by SiO_2 coating.[19]

Figure 4 shows the TEM images of the coated nanofibers before and after annealing. SiO_2 was easily coated on VO_2(A)

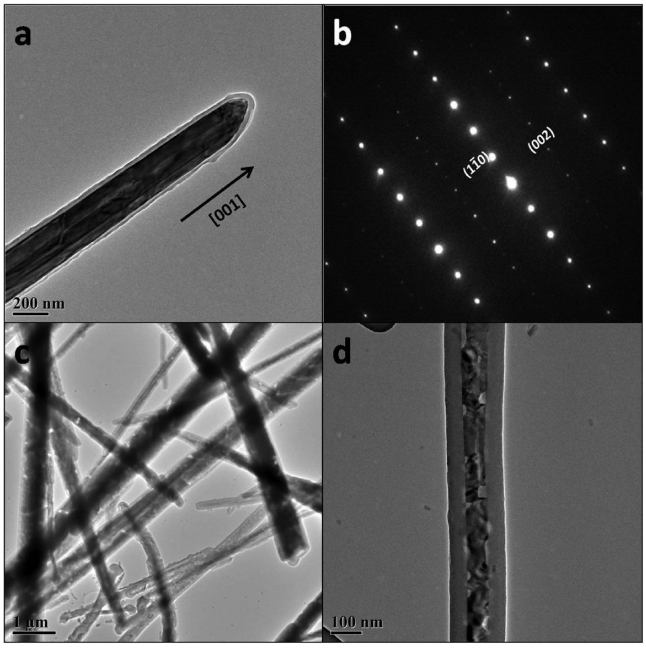

Figure 4. (a, b) TEM image and SAED pattern of VO_2(A)@SiO_2 nanofibers. (c, d) TEM images of VO_2(M)@SiO_2 nanofibers.

nanofibers with an uniform thickness without any surface modification as shown in Figure.4a. The selected area electron diffraction pattern (SAED) of the VO_2(A)@SiO_2 was shown in Figure 4b, indicating that the VO_2(A) nanofibers were single crystals which grown along the [001] crystal orientation. The space group of the VO_2(A) fibers was confirmed to be *P*4/*ncc* rather than $P4_2/ncm$ by comparing the SAED with that in ref 14. TEM images c and d in Figure 4 show the TEM images of the VO_2(M)@SiO_2 after annealing, exhibiting their fibrous structure, and Figure 4d further demonstrates the core−shell fine structure. The whole fiber maintained its original shape because of the protection effect of the inert SiO_2 shell, because strain and distortion of the VO_2(M) was limited by the SiO_2 shell.

Interestingly, it was found in Figure 4d that pores were inside VO_2(M)@SiO_2 nanofiber between the core and the shell. It has been pointed out earlier that the pores are the results of volume shrinkage of the nanofibers, while the thermal expansion of SiO_2 was unobvious during annealing. The porous VO_2(M)@SiO_2 structure is considered to have positive effects for the smart window performance of VO_2(M). The pores as well as the SiO_2 shell decrease the effective refractive index of VO_2(M), contributing to an increased transmittance. Besides, the introduction of pores increases the thermal insulation ability of the VO_2(M).

DSC was utilized to investigate the transition behavior of the nanofibers. Figure.5 shows the DSC curves of the VO_2(M) and

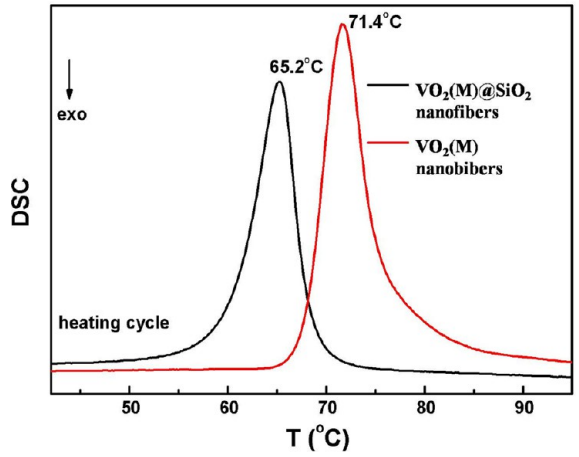

Figure 5. DSC curves of VO_2(M) nanofibers and VO_2(M)@SiO_2 nanofibers.

VO_2(M)@SiO_2. The uncoated VO_2(M) exhibits a sharp enthalpy change during the phase transition with a value of 37.91 J/g, and the transition temperature upon heating (the endothermic peak position) was 71.4 °C, comparable to 68 °C of the bulk crystal. However, the VO_2(M)@SiO_2 exhibits a slightly reduced enthalpy change due to a smaller VO_2(M) weight proportion, and the phase transition temperature was decreased to 65.2 °C, probably due to the stress and strain in the confined VO_2(M) grains.

The fibrous feature of VO_2(A)@SiO_2 nanofibers with large aspect ratio allows them to be easily arranged into a self-supporting film by filtration in the similar way to other 1D materials such as carbon nanotubes and silver nanofibers[20,21] (the fabrication processes were shown in Figure in the Supporting Information). SEM images of the self-supporting film shown in Figure S3 in the Supporting Information indicated that the film was loose and composed by the overlapped nanofibers. Optical measurement was done directly on the fibrous film with a spectrometer as the sketch map was shown in Figure 6a. Figure 6b showed the spectral transmittance at 25 and 90 °C, respectively. As expected, the film exhibited a high transmittance at 25 °C following the typical semiconductor behavior, while it showed a largely reduced transmittance at 90 °C particularly in the infrared region, which is the characteristic of metallic state. The difference in IR transmittance at 2500 nm between the two temperatures was more than 30%, indicating an excellent thermochromic property of the fibers. Furthermore, the film showed a relatively high visible transmittance over 50% probably due to the fibrous structure with small fiber radius and interfiber spaces for light transmission. Interestingly, the film does not show the intrinsic yellow color of VO_2(M), rather being grayish because of a structure effect, which will be beneficial for visual experience when applied in smart window or smart curtains.

4. CONCLUSION

In summary, we prepared VO_2(A) nanofibers by reduction of NH_4VO_3 with different reducing agents. Hydrothermal reaction conditions were varied to study their influence on the final product. VO_2(A) nanofibers were coated by SiO_2 to keep their morphology during heat treatment. VO_2(M)@SiO_2 nanofibers

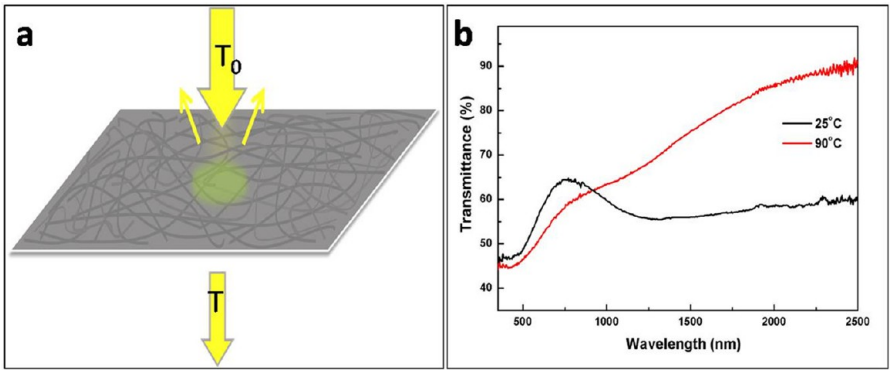

Figure 6. (a) Sketch map of the self-supporting thermochromic films composed of VO_2(M)@SiO_2 nanofibers when it was tested optical property. (c) Transmittance spectra of the self-supporting film composed of VO_2(M)@SiO_2 nanofibers.

were obtained by annealing and made into a self-supporting film with excellent thermochromic property by filtration.

■ ASSOCIATED CONTENT

Supporting Information

Additional table and figures (PDF). This material is available free of charge via the Internet at http://pubs.acs.org.

■ AUTHOR INFORMATION

Corresponding Author

*E-mail: p-jin@mail.sic.ac.cn.

Notes

The authors declare no competing financial interest.

■ ACKNOWLEDGMENTS

This study was financially supported by the National Natural Science Foundation of China (NSFC, 51032008, 51272273, 51102270, 51272271, 51172265), the National Key Basic Research Program (NKBRP, 2009CB939904), and the high-tech project of MOST (2012AA030605, 2012BAA10B03).

■ REFERENCES

(1) Morin, F. J. *Phys. Rev. Lett.* **1959**, *3*, 34−36.
(2) Goodenou, Jb. *J. Solid State Chem.* **1971**, *3*, 490−&.
(3) Gao, Y.; Luo, H.; Zhang, Z.; Kang, L.; Chen, Z.; Du, J.; Kanehira, M.; Cao, C. *Nano Energy* **2012**, *1*, 221−246.
(4) Kakiuchida, H.; Jin, P.; Tazawa, M. *Thin Solid Films* **2008**, *516*, 4563−4567.
(5) Xu, G.; Jin, P.; Tazawa, M.; Yoshimura, K. *Sol. Energy Mater. Sol. Cells* **2004**, *83*, 29−37.
(6) Vernardou, D.; Pemble, M. E.; Sheel, D. W. *Chem Vapor Depos* **2006**, *12* (5), 263−274.
(7) Zhang, Z.; Gao, Y.; Chen, Z.; Du, J.; Cao, C.; Kang, L.; Luo, H. *Langmuir: the ACS journal of surfaces and colloids* **2010**, *26*, 10738−44.
(8) Patridge, C. J.; Whittaker, L.; Ravel, B.; Banerjee, S. *J. Phys. Chem. C* **2012**, *116*, 3728−3736.
(9) Wei, J.; Ji, H.; Guo, W.; Nevidomskyy, A. H.; Natelson, D. *Nat.Nanotechnol.* **2012**, *7*, 357−362.
(10) Cao, C.; Gao, Y.; Luo, H. *J. Phys. Chem. C* **2008**, *112*, 18810−18814.
(11) Gao, Y.; Wang, S.; Kang, L.; Chen, Z.; Du, J.; Liu, X.; Luo, H.; Kanehira, M. *Energy Environ. Sci.* **2012**, *5*, 8234.
(12) Li, J.; Liu, C.-y.; Mao, L.-j. *J. Solid State Chem.* **2009**, *182*, 2835−2839.
(13) Zhang, K. F.; Liu, X.; Su, Z. X.; Li, H. L. *Mater. Lett.* **2007**, *61*, 2644−2647.
(14) Gao, Y.; Cao, C.; Dai, L.; Luo, H.; Kanehira, M.; Ding, Y.; Wang, Z. L. *Energy Environ. Sci.* **2012**, *5*, 8708.
(15) Zhang, W.; Shi, L.; Tang, K.; Yu, Y. *Chem. Lett.* **2012**, *41*, 104−106.
(16) Ji, S.; Zhang, F.; Jin, P. *J. Phys. Chem. Solids* **2012**, *73*, 762−769.
(17) Dai, L.; Gao, Y.; Cao, C.; Chen, Z.; Luo, H.; Kanehira, M.; Jin, J.; Liu, Y. *RSC Adv.* **2012**, *2*, 5265.
(18) Yamazaki, S.; Li, C.; Ohoyama, K.; Nishi, M.; Ichihara, M.; Ueda, H.; Ueda, Y. *J. Solid State Chem.* **2010**, *183*, 1496−1503.
(19) Gao, Y.; Wang, S.; Luo, H.; Dai, L.; Cao, C.; Liu, Y.; Chen, Z.; Kanehira, M. *Energy Environ. Sci.* **2012**, *5*, 6104.
(20) Wu, Z.; Chen, Z.; Du, X.; Logan, J. M.; Sippel, J.; Nikolou, M.; Kamaras, K.; Reynolds, J. R.; Tanner, D. B.; Hebard, A. F.; Rinzler, A. G. *Science* **2004**, *305*, 1273−6.
(21) De, S.; Higgins, T. M.; Lyons, P. E.; Doherty, E. M.; Nirmalraj, P. N.; Blau, W. J.; Boland, J. J.; Coleman, J. N. *ACS Nano* **2009**, *3*, 1767−1774.